

Néel Temperature of Quasi-Low-Dimensional Heisenberg Antiferromagnets

C. Yasuda¹, S. Todo², K. Hukushima³, F. Alet^{4,5}, M. Keller⁴, M. Troyer^{4,5}, and H. Takayama⁶

¹ *Department of Physics, Aoyama Gakuin University, Sagamihara 229-8558, Japan*

² *Department of Applied Physics, University of Tokyo, Tokyo 113-8656, Japan*

³ *Department of Basic Science, University of Tokyo, Tokyo 153-8902, Japan*

⁴ *Theoretische Physik, Eidgenössische Technische Hochschule, CH-8093 Zürich, Switzerland*

⁵ *Computational Laboratory, Eidgenössische Technische Hochschule, CH-8092 Zürich, Switzerland and*

⁶ *Institute for Solid State Physics, University of Tokyo, Kashiwa 277-8581, Japan*

(Dated: February 19, 2019)

The Néel temperature, T_N , of quasi-one- and quasi-two-dimensional antiferromagnetic Heisenberg models on a cubic lattice is examined by large-scale Monte Carlo simulations. Its dependence on the strength of inter-chain or inter-layer coupling, J' , is determined down to very small $J'/J \simeq 10^{-3}$, with J being the intra-chain or intra-layer coupling strength. It is found that T_N in the quasi-low-dimensional regime obeys a modified random-phase approximation-like relation with an effective renormalized coordination number. These numbers turn out to be the same for spin $S = 1/2$ and the classical limit $S = \infty$. Empirical formulae describing T_N for a wide range of J' and useful for the analysis of experimental measurements are presented.

While genuinely one-dimensional (1D) and two-dimensional (2D) antiferromagnetic Heisenberg (AFH) models cannot display long-range order (LRO) except at zero temperature [1], weak inter-chain or inter-layer couplings, J' , which always exist in real materials, lead to a finite Néel temperature T_N . So far, the J' -dependence of T_N was calculated by exactly treating effects of the strong interaction J in the 1D or 2D system, but using mean-field approximations for the inter-chain and inter-layer coupling J' [2]. Recently, more advanced theories of the latter effects have been proposed [3, 4], and the results have been compared with the experimental observations on quasi-1D (Q1D) antiferromagnets, e.g., Sr_2CuO_3 [5]. In view of the importance of experimentally well-studied quasi-2D (Q2D) antiferromagnets as undoped parent compounds of the high-temperature superconductors, accurate and unbiased numerical results for Q1D and Q2D AFH models are strongly desired. In a recent work along this line, Sengupta *et al.* [6] have demonstrated peculiar temperature dependences of the specific heat in the quantum Q2D AFH model.

Here we calculate the Néel temperature T_N as a function of J' and the spin size S in fully three-dimensional (3D) classical and quantum Monte Carlo (MC) simulations of coupled-chains and coupled-planes. We compare the MC results with theoretical predictions and find that they are well described for small J'/J by a modified random-phase approximation (RPA), with a renormalized coordination number. The latter is defined by

$$\zeta(J') \equiv \frac{1}{J' \chi_s(T_N(J'))}, \quad (1)$$

where $\chi_s(T)$ is the staggered susceptibility of the 1D or 2D model at temperature T . This quantity is z_d if T_N is determined in a simple RPA [2], where z_d is the coordination number in the inter-chain or inter-layer directions: $z_1 = 4$ and $z_2 = 2$ for the Q1D and Q2D systems, respectively. Our main result is that $\zeta(J')$ is constant

$\zeta(J') \approx \zeta_d$ for $J' \ll J$ but the constant differs from the RPA result z_d , i.e., $\zeta_1 = 0.695z_1$ and $\zeta_2 = 0.65z_2$. Surprisingly the constants are the same for the $S = 1/2$ quantum and the $S = \infty$ classical models within the present numerical accuracy. Our quantum Q1D (q-Q1D) result agrees even quantitatively with that of Irkhin and Katanin (IK) [3] who have developed a modified, self-consistent, RPA theory for the q-Q1D model, and have derived the condition for $T_N(J')$ at small J'/J ,

$$\zeta(J') = k z_d, \quad (2)$$

as the first order contribution in a $1/z_1$ expansion, where $k \simeq 0.70$ for $d = 1$.

In the present work we also propose empirical formulae for $T_N(J')$ in a wide range of J' , which are useful to analyze experimental results on infinite-layer antiferromagnets such as $\text{Ca}_{0.85}\text{Sr}_{0.15}\text{CuO}_2$ [7], $(5\text{CAP})_2\text{CuBr}_4$ and $(5\text{MAP})_2\text{CuBr}_4$ [8]. These allow the strength of inter-chain and inter-layer coupling J' to be determined from experimental measurements of T_N .

Model and numerical methods.— The Hamiltonian of the Q1D and Q2D AFH models is defined on an anisotropic simple cubic lattice:

$$\mathcal{H} = \sum_{i,j,k} (J_x \mathbf{S}_{i,j,k} \cdot \mathbf{S}_{i+1,j,k} + J_y \mathbf{S}_{i,j,k} \cdot \mathbf{S}_{i,j+1,k} + J_z \mathbf{S}_{i,j,k} \cdot \mathbf{S}_{i,j,k+1}), \quad (3)$$

where the summation $\sum_{i,j,k}$ runs over all the lattice sites on an $L_x \times L_y \times L_z$ cubic lattice and $\mathbf{S}_{i,j,k}$ is the $S = 1/2$ spin operator at site (i, j, k) . We put $J_x = J_y = J$ and $J_z = J'$ for the Q2D model and $J_x = J_y = J'$ and $J_z = J$ for the Q1D model with $J > 0$ and $0 \leq J' \leq J$. For comparison, we also examine the classical limit $S = \infty$ of Eq. (3). Note that $JS(S+1)$ sets the energy scale in the classical model. In practice, we simulate a system of unit vectors, which is equivalent to fixing $JS(S+1)$ to unity.

TABLE I: Néel temperatures of the q-Q1D, c-Q1D, q-Q2D, and c-Q2D AFH models, normalized by $JS(S+1)$. The result for the classical system with $J'/J = 1$ is taken from Ref. [12].

J'/J	$T_N/JS(S+1)$			
	q-Q1D	c-Q1D	q-Q2D	c-Q2D
1	1.2589(1)	1.4429(1)	1.2589(1)	1.4429(1)
0.5	0.78997(8)	0.9317(1)	1.0050(4)	1.1733(1)
0.1	0.22555(3)	0.39551(8)	0.6553(4)	0.8526(1)
0.05	0.12171(5)	0.28377(4)	0.5689(2)	0.7797(1)
0.02	0.05258(1)	0.18361(3)	0.48463(8)	0.7115(1)
0.01	0.02768(1)	0.13157(2)	0.43515(6)	0.6731(2)
0.005		0.09393(2)	0.39513(4)	0.6419(2)
0.001		0.042547(6)	0.32571(8)	0.5858(4)

The MC simulations have been performed using the continuous-imaginary-time loop algorithm [9] for the quantum model (QMC) and the Wolff cluster algorithm [10] for the classical model (CMC). The AF correlation length ξ_α in each of the directions α ($= x, y, z$) are evaluated by the second-moment method [11] on lattices whose aspect ratio is chosen such that ξ_α/L_α does not depend on α in the vicinity of T_N . Explicitly, for the q-Q1D systems with $J'/J = 0.01, 0.05, 0.1$, and 0.5 , we set $L_z/L_x = 36$ ($L_z \leq 504$), 12 (384), 4 (200), and 2 (128), respectively, while for the quantum Q2D (q-Q2D) systems with $J'/J = 0.001, 0.005, 0.01$, and ≥ 0.02 , we set $L_x/L_z = 48$ ($L_x \leq 288$), 20 (240), 16 (192), and 1 (80), respectively. Then we determine T_N from finite-size scaling, looking for the best data collapse of ξ_α/L_α plotted versus $(T - T_N)L^{1/\nu}$ for different system sizes. We have fixed the exponent $\nu = 0.71$ [12] to the value of the 3D classical Heisenberg universality class. The values of T_N obtained for the q-Q1D and classical Q1D (c-Q1D) systems, and the q-Q2D and classical Q2D (c-Q2D) systems are listed in Table I.

Q1D systems.— We begin the presentation of the detailed results with the 1D models where the quantum effects are stronger than in the 2D models described later. While the classical 1D (c-1D) model shows LRO at $T = 0$, the ground state of the quantum 1D (q-1D) model has no LRO. Instead it is a gapless, critical state in the models with half-odd integer spins [13], and the gapful Haldane state [14] for the models with integer spins. Correspondingly, the staggered susceptibility χ_s diverges as T^{-2} in the limit $T \rightarrow 0$ for the classical model [15]:

$$\chi_s(T) = \frac{x}{3J} \frac{1 + 1/\tanh x - 1/x}{1 - 1/\tanh x + 1/x}, \quad (4)$$

with $x = JS(S+1)/T$, but it exhibits only a $1/T$ divergence with logarithmic corrections [16] for the $S = 1/2$ model:

$$\chi_s(T) = \frac{c_1}{T} \sqrt{\ln\left(\frac{\Lambda J}{T}\right) + \frac{1}{2} \ln \ln\left(\frac{\Lambda J}{T}\right)}. \quad (5)$$

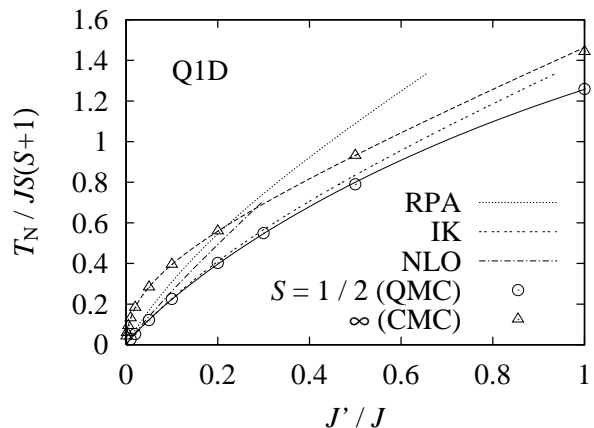


FIG. 1: J' -dependence of $T_N/JS(S+1)$ for the Q1D systems. The open symbols denote our numerical results for the $S = 1/2$ (circles) and $S = \infty$ (triangles) models. The error bar of each point is much smaller than the symbol size. The dashed curve passing through the $S = \infty$ data is obtained by Eq. (2) with the exact expression for χ_s (4). The solid curve denotes the proposed empirical formula (9). The other curves are results of various approximations discussed in the text.

The quantitative accuracy of this asymptotic expression for the quantum model is limited to a very low temperature range. We find that Eq. (5) with the constants c_1 and Λ derived field-theoretically [16] does not fit well to the numerically calculated χ_s in the temperature range of interest here. This fact has to be taken care of when we will further analyze $T_N(J')$ via $\zeta(J')$ in Eq. (1).

Due to the different functional forms of the quantum and classical susceptibilities, we observe in Fig. 1 that, at small J'/J , $T_N(J') \propto \sqrt{J'/J}$ for the classical $S = \infty$ model, while $T_N(J') \propto J'/J$ with logarithmic corrections for the quantum $S = 1/2$ model. Comparing the RPA result (Eq. (2) with $k = 1$ and $d = 1$) with the modified RPA one (Eq. (2) with $k \simeq 0.70$, denoted by IK), one can easily see that the latter describes $T_N(J')$ much better and is a fairly good description of $T_N(J')$ in the range $J'/J \lesssim 0.3$. This is further illuminated in Fig. 2 where the J' -dependence of $\zeta(J')$ in Eq. (1) is shown. The $\chi_s(T_N(J'))$ are obtained from QMC simulations interpolated near $T = T_N$ for the $S = 1/2$ model and from the exact expression (5) for the $S = \infty$ model. For $J'/J \leq 0.1$ we find for the q-Q1D model

$$\zeta(J') \approx \zeta_1 = 0.695z_1 \quad (6)$$

and conclude that, within the numerical accuracy of our simulation, the modified RPA is an appropriate quantitative description of the q-Q1D models with small J'/J . Interestingly the above equation also holds for the classical limit $S = \infty$ model with small J'/J . This is surprising, given the different behavior of $\chi_s(T)$ in the c-1D and q-1D models.

Comparing our results to the next leading order finite-

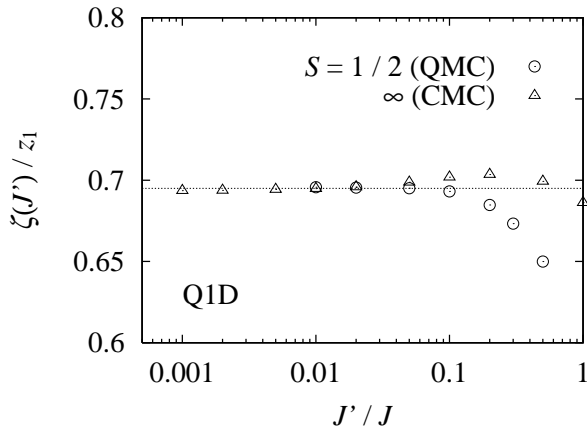


FIG. 2: J' -dependence of $\zeta(J')/z_1$ for the Q1D systems with $S = 1/2$ (circles) and $S = \infty$ (triangles). In both cases $\zeta(J')/z_1$ approaches a constant ($\simeq 0.695$), denoted by the dotted line, at small J'/J . The error bar of each point is smaller than the symbol size.

temperature perturbation theory [4] (NLO in Fig. 1) we do not find good agreement. This is most probably due to the fact that the NLO result is based on Eq. (5) which we already found to be inappropriate in the considered temperature range.

Q2D systems.— In both classical 2D (c-2D) and quantum 2D (q-2D) models, AF-LRO appears at $T = 0$, together with an exponential divergence of $\chi_s(T)$ in the limit $T \rightarrow 0$. In the c-2D system, χ_s is proportional to $T^3 \exp(4\pi J/T)$ at low temperatures [17] and our numerical results agree with previous simulations [18]. For the q-2D models, there is a similar exponential divergence at low temperatures in the renormalized classical regime of the non-linear σ model [19]:

$$\chi_s(T)J = c_2 T/J \exp(4\pi\rho_s/T), \quad (7)$$

where ρ_s is the spin stiffness and c_2 a constant. Our results again agree with previous extensive simulations [20].

The J' -dependences of T_N for the Q2D models are shown in Fig. 3 and we find that here – in contrast to the Q1D models – due to the similar functional forms of χ_s , $T_N(J') \propto -1/\ln(J'/J)$ at small J'/J both in the $S = 1/2$ and $S = \infty$ models. The reduction of T_N for the quantum model relative to that of the classical one is smaller here than in the Q1D models, since quantum fluctuations are less pronounced in two dimensions. Figure 4 shows that again for small J'/J the value $\zeta(J')$ is constant and the same for both the quantum and the classical models:

$$\zeta(J') \approx \zeta_2 = 0.65z_2. \quad (8)$$

A modified RPA-like form with a renormalized coordination number describes $T_N(J')$ much better than the simple RPA, though there is no analytic prediction for the value of ζ_2 available.

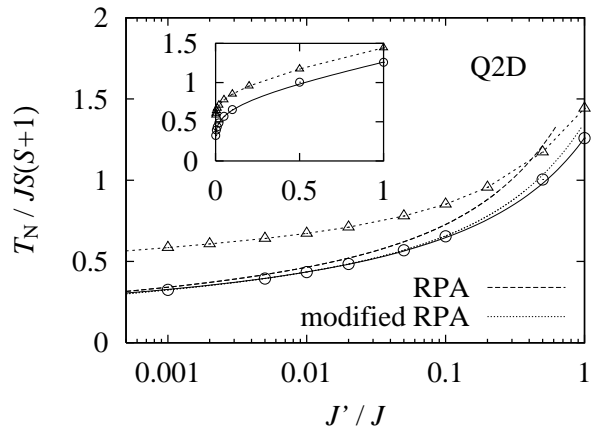


FIG. 3: J' -dependence of $T_N/JS(S+1)$ for the Q2D systems. The open symbols denote our numerical results for the $S = 1/2$ (circles) and $S = \infty$ (triangles) models. The error bar of each point is much smaller than the symbol size. The dashed (RPA) and dotted (modified RPA) curves are obtained from Eqs. (1) and (2) with $k = 1$ and $k = 0.65$, respectively. The solid curve denotes the proposed empirical formula (11), while the curve passing through the $S = \infty$ data is simply a guide for the eye. The inset shows the same data on a linear scale.

Empirical formulae.— Finally, we propose empirical formulae for $T_N(J')$ based on our QMC results in a wide range of couplings. For the q-Q1D systems we propose a modified RPA form based on Eqs. (5) and (6)

$$\frac{J'}{J} = \frac{T_N/J}{4c\sqrt{\ln(\frac{\lambda J}{T_N}) + \frac{1}{2}\ln\ln(\frac{\lambda J}{T_N})}}, \quad (9)$$

but with modified values of the constants with $c = 0.233(6)$ and $\lambda = 2.6(3)$. These values are chosen to reproduce not $\chi_s(T)$ but $T_N(J')$ in a wide range of J' . The formula describes $T_N(J')$ very well in the whole range of J'/J as shown by the solid curve in Fig. 1. It can be used to analyze experimental results, e.g. to obtain $J'/J \simeq 0.0007$ for Sr_2CuO_3 from $T_N/J \simeq 0.002$ [5].

For the q-Q2D system one can again try a modified RPA form, derived from Eq. (8) combined with the asymptotic expression (7)

$$\frac{T_N}{J} = \frac{4\pi\rho_s/J}{b - \ln(J'/J) - \ln(T_N/J)}, \quad (10)$$

with $b = -\ln(\zeta_2 c_2)$. Instead of this expression, expected to work at very low temperatures, we find that the following simpler expression describes the T_N better in the coupling range $0.001 \leq J'/J \leq 1$ (see Fig. 3):

$$\frac{T_N}{J} = \frac{4\pi\rho_s/J}{b - \ln(J'/J)}, \quad (11)$$

with $\rho_s/J = 0.183(1)$ and $b = 2.43(1)$. Table II shows inter-layer couplings J' estimated using this equation for a number of infinite-layer materials. For other materials,

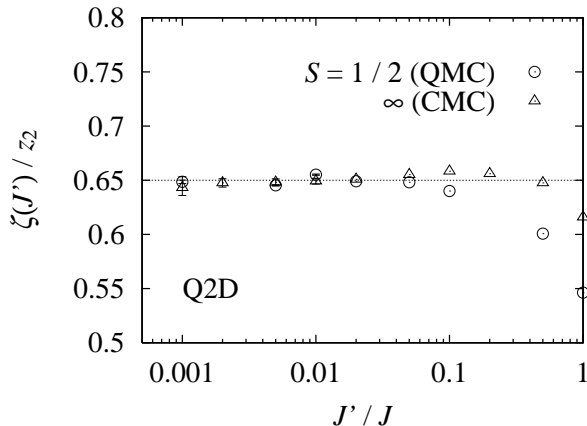


FIG. 4: J' -dependence of $\zeta(J')/z_2$ for the Q2D systems with $S = 1/2$ (circles) and $S = \infty$ (triangles). In both cases $\zeta(J')/z_2$ approaches a constant ($\simeq 0.65$), denoted by the dotted line, at small J'/J . The error bar of each point is smaller than the symbol size unless given explicitly.

TABLE II: Inter-layer coupling J' estimated by Eq. (11) for various infinite-layer compounds. The Néel temperatures T_N , the intra-layer couplings J , and their ratio estimated by the experiments are also listed.

Compound	T_N	J	T_N/J	J'/J
$\text{Ca}_{0.85}\text{Sr}_{0.15}\text{CuO}_2$ [7]	537K	1535K	0.35	0.016
$(5\text{CAP})_2\text{CuBr}_4$ [8]	5.08K	8.5K	0.60	0.24
$(5\text{MAP})_2\text{CuBr}_4$ [8]	3.8K	6.5K	0.58	0.22
$(5\text{CAP})_2\text{CuCl}_4$ [8]	0.74K	1.14K	0.64	0.33
$(5\text{MAP})_2\text{CuCl}_4$ [8]	0.44K	0.76K	0.57	0.21

like the very good Q2D system $\text{Sr}_2\text{CuO}_2\text{Cl}_2$ [21] a similar formula is harder to obtain since in these single-layer compounds the inter-layer coupling is frustrated and the ordering transition is driven by exchange anisotropies instead of inter-layer coupling.

To conclude, we have determined, by high-precision Monte Carlo simulations, the Néel temperatures of quantum ($S = 1/2$) and classical ($S = \infty$) quasi-one- and quasi-two-dimensional Heisenberg antiferromagnets. Besides finding empirical formulae for T_N , we observe that a modified RPA theory succeeds in quantitatively describing the quasi-one-dimensional system when combined with our numerically determined staggered susceptibility. Furthermore, at small J' the renormalized coordination number, $\zeta(J')$, defined by Eq. (1), is found to be the same for the $S = 1/2$ and the $S = \infty$ systems. It will be of interest to check whether these results also hold for the $S = 1$ system where the isolated quantum chain has a gapful ground state [14]. Although no modified RPA theory exists for the quasi-two-dimensional models, we find similar behavior to the quasi-one-dimensional models: a modified RPA is appropriate at small couplings with a common renormalized coordination number for

the quantum and the classical systems. It will also be interesting to study in future simulations the effects of spin anisotropies on the Néel temperature.

We acknowledge fruitful discussions with C.P. Landee and thank M. Bocquet for useful discussions and for sending his NLO results. Most of the numerical calculations have been performed on the SGI 2800 at Institute for Solid State Physics, University of Tokyo. The program is based on ‘Looper version 2’ developed by S.T. and K. Kato and ‘PARAPACK version 2’ by S.T. This work is supported by Grant-in-Aid for Scientific Research Programs (#12640369, #15740232) and 21st COE Program from the Ministry of Education, Science, Sports, Culture and Technology of Japan, and by the Swiss National Science foundation.

- [1] N. D. Mermin and H. Wagner, Phys. Rev. Lett. **17**, 1133 (1966).
- [2] D. J. Scalapino, Y. Imry, and P. Pincus, Phys. Rev. B **11**, 2042 (1975); H. J. Schulz, Phys. Rev. Lett. **77**, 2790 (1996).
- [3] V. Yu. Irkhin and A. A. Katanin, Phys. Rev. B **61**, 6757 (2000).
- [4] M. Bocquet, Phys. Rev. B **65**, 184415 (2002).
- [5] A. Keren *et al.*, Phys. Rev. B **48**, 12926 (1993); T. Ami *et al.*, *ibid.* **51**, 5994 (1995).
- [6] P. Sengupta, A. W. Sandvik, and R. R. P. Singh, preprint cond-mat/0306046.
- [7] T. Siegrist *et al.*, Nature (London), **334**, 231 (1988); D. Vakhnin *et al.*, Phys. Rev. B **39**, 9122 (1989); Y. Tokura *et al.*, *ibid.* **41**, 11657 (1990).
- [8] F. M. Woodward *et al.*, Phys. Rev. B **65**, 144412 (2002).
- [9] H. G. Evertz, G. Lana, and M. Marcu, Phys. Rev. Lett. **70**, 875 (1993); B. B. Beard and U.-J. Wiese, *ibid.* **77**, 5130 (1996); S. Todo and K. Kato, *ibid.* **87**, 047203 (2001).
- [10] U. Wolff, Phys. Rev. Lett. **62**, 361 (1989); Nucl. Phys. B **322**, 759 (1989).
- [11] F. Cooper, B. Freedman, and D. Preston, Nuc. Phys. B **210** [FS6], 210 (1982).
- [12] K. Chen, A. M. Ferrenberg, and D. P. Landau, Phys. Rev. B **48**, 3249 (1993).
- [13] L. Hulthén, Arkiv. Mat. Astron. Fysik **26A**, No. 11 (1938); J. des Cloizeaux and J. J. Pearson, Phys. Rev. **128**, 2131 (1962).
- [14] F. D. M. Haldane, Phys. Lett. **93A**, 464 (1983); Phys. Rev. Lett. **50**, 1153 (1983).
- [15] T. Nakamura, J. Phys. Soc. Jpn. **7**, 264 (1952); M. E. Fisher, Amer. J. Phys. **32**, 343 (1964).
- [16] V. Barzykin, Phys. Rev. B **63**, 140412 (2001).
- [17] E. Brézin and J. Zinn-Justin, Phys. Rev. B **14**, 3110 (1976).
- [18] J. Apostolakis, C. F. Baillie, and G. C. Fox, Phys. Rev. D **43**, 2687 (1991).
- [19] S. Chakravarty, B. I. Halperin, and D. R. Nelson, Phys. Rev. B **39**, 2344 (1989); P. Hasenfratz and F. Niedermayer, Z. Phys. B **92**, 91 (1993).
- [20] J-K. Kim and M. Troyer, Phys. Rev. Lett. **80**, 2705 (1998); B. B. Beard *et al.*, *ibid.* **80**, 1742 (1998).
- [21] M. Greven *et al.*, Z. Phys. B **96**, 465 (1995).